RESEARCH

Theoretical aspects of interaction of the anticancer drug cytarabine with human serum albumin

Maryam Amirinasab[1] · Maryam Dehestani[1]

Abstract
Despite diagnostic and therapeutic methods, cancer is a major cause of death worldwide. Since anticancer drugs affect both normal and cancer cells, targeted drug delivery systems can play a key role in reducing the destructive effects of anticancer drugs on normal cells. In this regard, the use of stimulus-sensitive polymers has increased in recent years. This study has attempted to investigate interaction of the anticancer drug cytarabine with a stimuli-sensitive polymer, human serum albumin (HSA), one of the most abundant protein in blood plasma, via computational methods at both body temperature and tumor temperature. For this purpose, molecular docking was performed using Molegro virtual Docker software to select the best ligand in terms of binding energy to simulate molecular dynamics. Then, molecular dynamics simulation was performed on human serum albumin with code (1Ao6) and cytarabine with code (AR3), using Gromacs software and the results were presented in the graphs. The simulations were performed at 310 K (normal cell temperature) and 313 K (cancer cell temperature) in 100 ns. Results showed drug release occurred at a temperature of 313 K. These findings demonstrated the sensitivity of human serum albumin to temperature.

Keywords Human serum albumin · Cytarabine · Targeted drug delivery · Molecular dynamics simulation · Molecular docking

Introduction

Cancer is caused by a defect in oncogenes and tumor suppressor genes that can affect abnormal cell growth and increase cell division [1–4]. Diagnosis and treatment of cancer are possible by stabilizing cell growth and correcting the damaging mechanisms of genes, cutting off blood supply to cells or destroying them [5, 6]. Common methods of cancer diagnosis are performed by X-ray, CT scan, or cell biopsy, which is not very sensitive [7]. Because the cancer diagnosis in the early stages is very important in cancer treatment, these methods are not effective [8]. Therefore, the use of nanotechnology in the diagnosis and treatment of cancer has increased greatly in recent decades. Nanostructures, like quantum dots, are nanoscale devices that have the ability to enter multimicron cells and access DNA molecules for identification of genetic defense in high sensitivity [9]. Nanotechnology can target specific cells and deliver drugs to destroy them by producing therapeutic tools. Therefore, the two main advances in nanotechnology in chemotherapy are the detection of cancer cells and the ability of nanoparticles to reach the tumor site [10, 11]. At the nanoscale, particles act so that the properties of materials change and show special optical, electronic, and structural properties [12, 13]. In modern drug delivery, using these features, nanoparticles are engineered to deliver high doses of the drug to the tumor site without damaging normal cells [14].

In recent years, there has been significant growth in the development of delivery systems based on stimulus-responsive polymers [15]. These polymers can convert the effect of a stimulus into a response. Some of these polymers can respond to several stimuli [16–18]. In addition, their structural properties, such as their flexibility and resemblance to the body's natural tissues, and the presence of numerous functional groups have made them very important carriers [19–21]. Albumin is also a stimulus-responsive protein that has been

✉ Maryam Dehestani
dehestani@uk.ac.ir

Maryam Amirinasab
ma.amiri.r@gmail.com

1 Department of Chemistry, Shahid Bahonar University of Kerman, Kerman, Iran

used as a carrier in this study. Human serum albumin (HSA) is a transport protein and the most abundant protein in the blood serum, which has received much attention since the early twentieth century [15, 22–24]. HSA consists of a 585-amino acid polypeptide sequence of distinct sequence, of which 17 pairs of disulfide bridges are free cysteine and tryptophan. It consists of three identical alpha spiral subdomains (I, II, and III). In addition, a domain has two subdomains marked with A and B [25–28]. It has ~67 kDa weight and its average half-life under normal conditions is 19 days [29]. This half-life converts albumin into an attractive carrier to enhance and improve the pharmacokinetic properties of cancer agents [30–35]. In addition to being the most important transporter of fatty acids and drugs, this protein also acts as a catalyst in the hydrolysis of esters and hopes and phosphates [36, 37]. In addition, albumin itself has a therapeutic role and is used in various formulations to carry pharmacological and diagnostic agents [38]. Furthermore, there are other benefits, including [23, 39, 40]: (i) it is the most important protein of blood plasma, so it has special physiological importance and many functions; (ii) because there are large amounts of it in the body, therefore, if a significant amount of it is injected into the body, it will not cause any side effects; (iii) albumin is extracted from the blood of blood donors, so its source is easy to access; and (iv) albumin is nontoxic and biocompatible. When broken down in the body, its building blocks, the amino acids, are used by the surrounding tissues to make protein. (v) Due to different functional groups, it is possible to bind to significant amounts of the drug; (vi) it is an acidic, highly soluble, desirable surface modification characteristics, stable protein, and it is very flexible. This feature is an important advantage in the physiological environment and outside the body.

The drug examined in this study is cytarabine (cytosine arabinoside, Ara-C,1–3-D arabinofuranosylcytosine) which was synthesized in 1959 [41]. The structure of cytarabine is shown in Fig. 1. Cytarabine with the molecular formula $C_9H_{13}N_3O_5$, is an anticancer drug that is mostly used in treating leukemia [42, 43]. It is a modified analog of the cytidine metabolite with a modified sugar moiety (arabinose instead of ribose) [44]. Cytarabine is converted to intracellular triphosphate and competes with cytidine to combine with DNA [45]. Because arabinose sugar three

dimensionally prevents the molecule from circulating inside DNA, DNA replication stops, especially in the S phase of the cell cycle. As a result, it reduces DNA replication and repair [44–49].

In this study, we investigate the interaction of the anticancer drug cytarabine using computational methods at both body temperature and tumor temperature. The computational techniques used in this work are molecular docking and molecular dynamics simulation. In recent years, these methods were also applied to discover the interaction of drug with proteins of coronavirus-2 (SARS CoV-2). [50–54].

Theoretical section

We have determined the pharmacokinetic characteristic (ADMET) for cytarabine including absorption, distribution, metabolism, excretion, and toxicity via the pkCSM (predicting small-molecule pharmacokinetic properties via graph-based signatures) website [55]. These data are given in Table 1.

The structure of human serum albumin protein (HSA) with code (1AO6) was obtained from the Protein Data Bank (http://www.rcsb.org/pdb). In addition, the drug structure under study was also received from the Drug Bank database with the code (AR3). Crystalline water molecules were removed from the protein structure, and protein and drug files were given to the Molegro Virtual Docker software for molecular docking. Using molecular docking, cases such as the binding energy and the important residues of the protein involved in the binding and the interaction modes between a ligand and protein can be investigated [56].

After the docking calculation, the generated files are displayed in the poses all sections. Among them, the conformation with the lowest binding energy (negative energy) was selected as the input to simulate molecular dynamics. In this study, the Gromacs 19.1 package (www.gromacs.org) was used throughout the simulation. Amber03 force field was selected, and the drug topology was received from the ACPYPE server (http://webapps.ccpn.ac.uk/acpype). The simulation box was designed as a cuboid of $13.879 \times 13.879 \times 13.879$ nm^3. The protein has been placed at the center of the box; the box was filled with water molecules. Minimizing energy is an important step in improving molecular structures before molecular dynamics simulation. Equilibration was performed in canonical (NVT) and isothermal–isobaric (NPT) ensembles with a step number of 500,000 for 1 ns. Then, the production step was performed with step number 50,000,000 for 100 ns. Finally, the leapfrog algorithm was used to solve the equations of motion. All stages were examined at two different temperatures 310 K and 313 K, with a Brendsen thermostat.

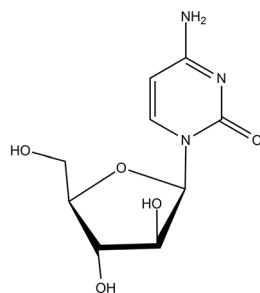**Fig. 1** The molecular structure of cytarabine

Table 1 The properties of ADMET for cytarabine

Properties		Units
Absorption		
Water solubility	− 1.689	Numeric (log mol/L)
Caco2 permeability	0.025	Numeric (log Papp in 10^{-6} cm/s)
Intestinal absorption (human)	43.155	Numeric (% absorbed)
Skin Permeability	− 2.745	Numeric (log Kp)
P-glycoprotein substrate	No	Categorical (yes/no)
P-glycoprotein I inhibitor	No	Categorical (yes/no)
P-glycoprotein II inhibitor	No	Categorical (yes/no)
Distribution		
VDss (human)	− 0.025	Numeric (log L/kg)
Fraction unbound (human)	0.765	Numeric (Fu)
BBB permeability	− 0.97	Numeric (log BB)
CNS permeability	-4.023	Numeric (log PS)
Metabolism		
CYP2D6 substrate	No	Categorical (yes/no)
CYP3A4 substrate	No	Categorical (yes/no)
CYP1A2 inhibitor	No	Categorical (yes/no)
CYP2C19 inhibitor	No	Categorical (yes/no)
CYP2C9 inhibitor	No	Categorical (yes/no)
CYP2D6 inhibitor	No	Categorical (yes/no)
CYP3A4 inhibitor	No	Categorical (yes/no)
Excretion		
Total clearance	0.562	Numeric (log mL/min/kg)
Renal OCT2 substrate	No	Categorical (yes/no)
Toxicity		
AMES toxicity	No	Categorical (yes/no)
Max. tolerated dose (human)	1.108	Numeric (log mg/kg/day)
hERG I inhibitor	No	Categorical (Yes/No)
hERG II inhibitor	No	Categorical (Yes/No)
Oral rat acute toxicity (LD50)	2.196	Numeric (mol/kg)
Oral rat chronic toxicity (LOAEL)	2.85	Numeric (log mg/kg_bw/day)
Hepatotoxicity	No	Categorical (yes/no)
Skin sensitization	No	Categorical (yes/no)
T. pyriformis toxicity	0.284	Numeric (log μg/L)
Minnow toxicity	3.675	Numeric (log mM)

Results and discussions

Molecular docking

Molecular docking of human serum albumin code 1Ao6 with anticancer drug cytarabine code AR3 was performed after selecting 5 holes of protein and minimizing the system. At the end of the docking tab, the poses all sections of the results were reported in Table 2.

According to these results, the ligand named [00] c_1 [A].mol2 has shown a docking score of − 63.2161 kJ mol^{-1} (Table 2) and has the lowest binding energy and is located in part IIIA of the protein. So, this ligand was used for simulation. Figure 2 shows the complex created after docking.

The ligand is located in the most suitable protein cavity with the lowest binding energy. Figure 2b indicates that GLU 400, LEU 398, GLN 404, ARG 428, LYS 402, TYR

Table 2 Results of molecular docking

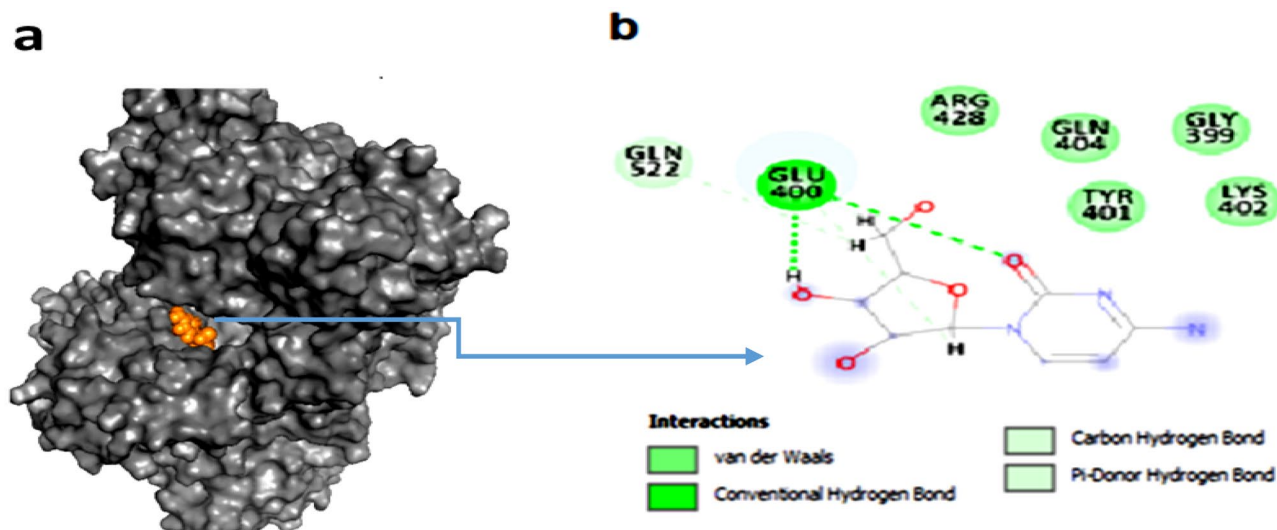| S. no	Mol Dock score (GRID) (kJ mol^{-1})	Mol Dock score (kJ mol^{-1})	Rerank score (kJ mol^{-1})
1	− 67.0796	− 63.2161	− 57.6600
2	− 62.9607	− 59.1377	− 51.7849
3	− 62.9465	− 53.6164	− 42.1171
4	− 62.8334	− 60.0685	− 54.4448
5	− 61.8851	− 52.3829	− 50.3197

Fig. 2 **a** Complex created after molecular docking. **b** Hydrogen and van der Waals bonds that formed between ligand and protein after docking of two molecules

401, GLY 399, GLN 526, and GLN 522 of the HSA protein take part in hydrogen and van der Waals bonds with the cytarabine atoms.

Molecular dynamics simulation

At first, in order to evaluate the stability of HSA protein structures at 310 K and HSA–cytarabine complex at 310 K and 313 K in simulation media, the mean squared deviation analysis (RMSD) was calculated (Fig. 3). This calculation

is the most reliable method of molecular dynamics simulation analysis and a criterion for the measure of the structural system's stability [57]. Figure 3 shows the RMSD diagram for protein at 310 K and the cytarabine protein complex at 310 K and 313 K. The slope of the diagram indicates the stability of the system during the simulation. An increase in the slope of the RMSD diagram from zero shows that the simulated model is unstable.

Most of the RMSD diagram changes during simulation for the HSA–cytarabine complex are at 313 K, which is in the range between 1.5 and 9 Å.

For HSA protein systems and the HSA-cytarabine complex at 310 K, these changes have been observed in the range
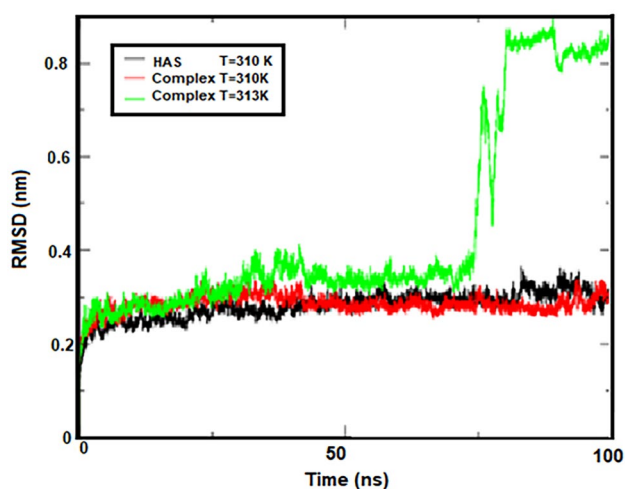

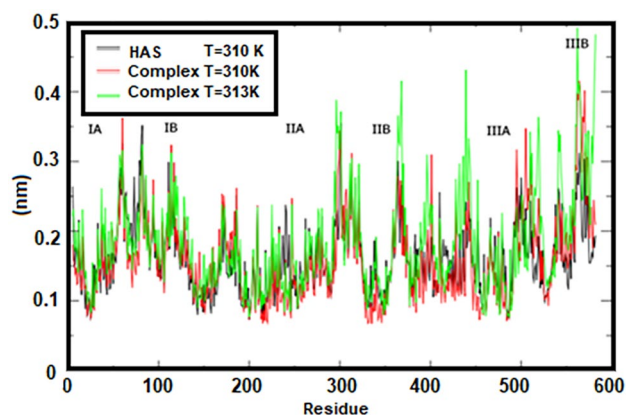**Fig. 3** RMSD for protein at 310 K and complex protein at 310 K and 313 K

Fig. 4 RMSF for protein at 310 K and complex protein at 310 K and 313 K by number of amino acids
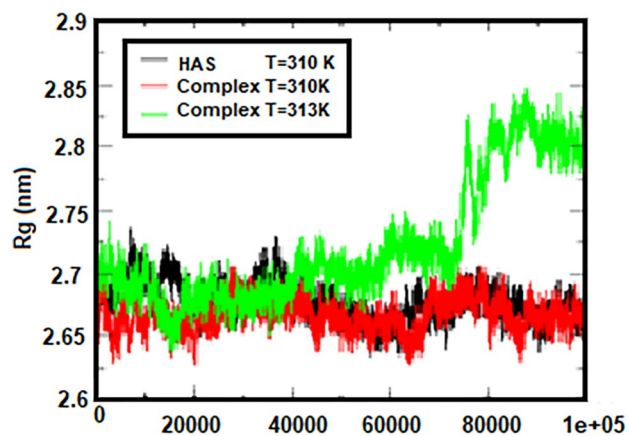
Radius of gyration (Total and around axes)

Fig. 5 The R_g corresponds to protein at 310 K and a complex at two temperatures of 310 K and 313 K

of 1.5 to 3.5 Å. As can be seen from Fig. 3, the HSA protein and the HSA–cytarabine complex reached to equilibrium at 310 K at 5 ns at the beginning of the simulation. The RMSD diagram of the HSA–cytarabine complex increases at 313 K over time and undergoes abrupt changes at 75 ns, indicating that the complex is unstable at temperatures close to

the temperature of the tumor and that cytarabine is isolated from the protein.

The motions of the HSA protein and HSA–cytarabine complex at 310 K and 313 K were analyzed using mean square root (RMSF) (Fig. 4). As shown in Fig. 4, the overall motions of the HSA protein and the complex at 310 K are very similar. Fluctuations for these two structures are observed in the range of 0.08 to 0.4 nm. The results clearly show that subdomains IIB and IIIB of the HSA protein have the most fluctuations, while subdomains IIA and IIIA have the least fluctuations. These results indicate that at the junction of cytarabine (IIIA) with human serum albumin at body temperature (310 K), a good interaction occurred and the drug remained in place during rigid simulation. Fluctuations related to the HSA–cytarabine complex at abnormal cell temperature (313 K) have occurred in the range of 0.08 to 0.5 nm. This indicates the instability of the HSA-cytarabine complex at 313 K and confirms the results of the RMSD analysis.

Gyrus radius (R_g) is one of the useful analyses obtained from the results of molecular dynamics simulations and has been selected as the first criterion to study the three-dimensional structure of the studied systems, because it can be directly compared to laboratory results. Furthermore, for large molecules such as proteins, the R_g is a good measure of the opening or closing branches. For example, the R_g value for HSA protein,

Fig. 6 Diagram of solvent availability level for **A** HSA protein at 310 K, **B** complex at 310 K, and **C** complex at 313 K
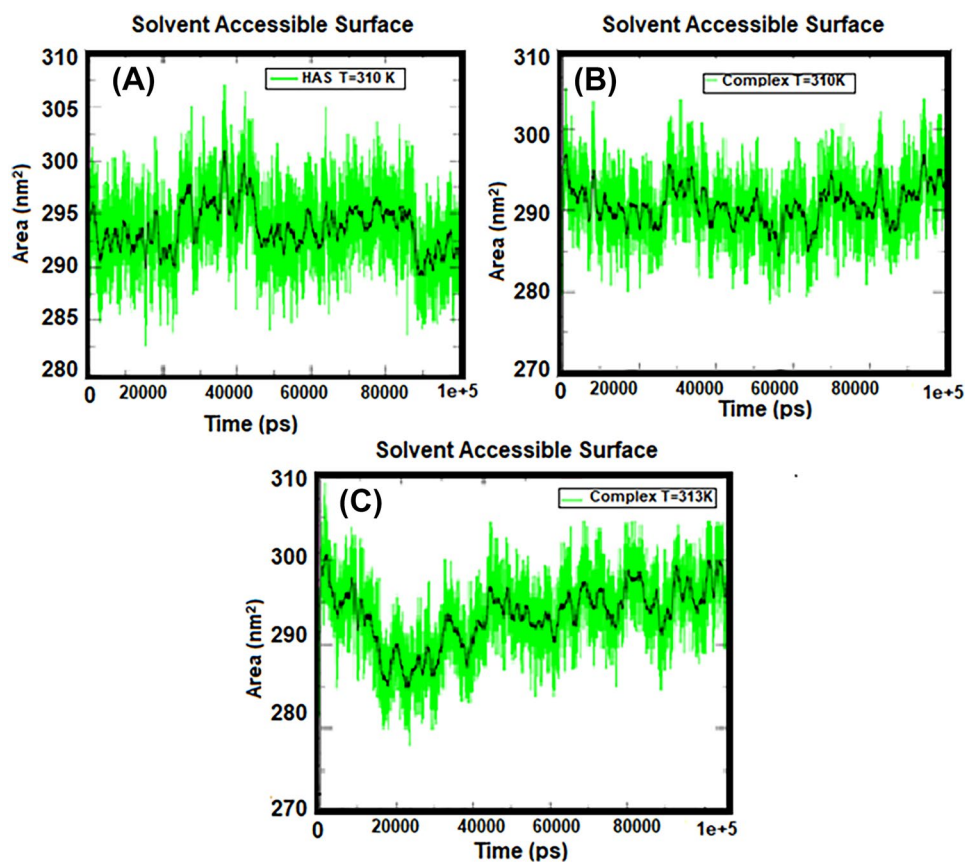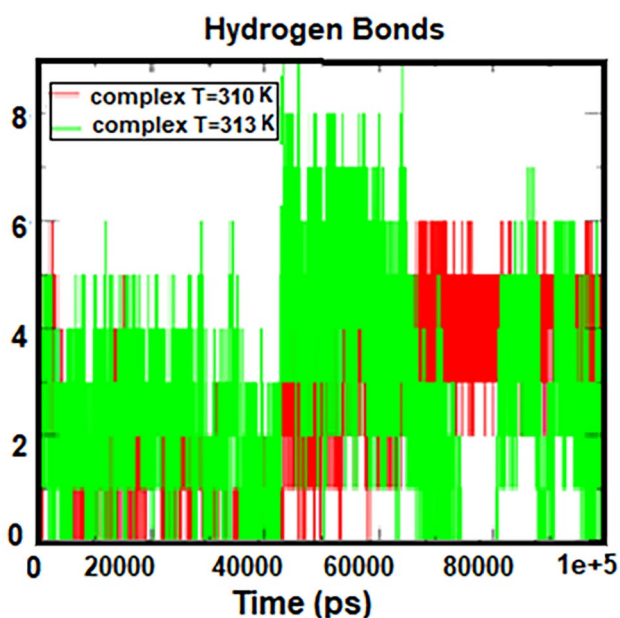
Fig. 7 Number of hydrogen bonds formed between HSA and cytarabine at 310 K and 313 K

which was experimentally measured in an aqueous solution, was reported to be 27.4 ± 0.34 Å [48].

In the present study, the R_g value for HSA protein was calculated to be 26.8 Å. This good agreement between theory and experiment indicates the accuracy of this work (MD) compared to the laboratory work. The evolution of the R_g diagrams during the simulation steps is shown in Fig. 5. Also, the R_g diagrams of the HSA protein and the complex at 310 K is in the agreement with the RMSD results and the stability of the systems. The results of these two graphs
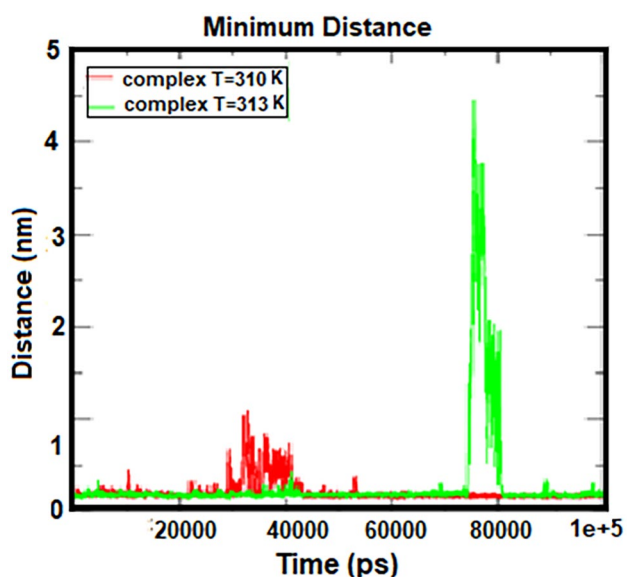

Fig. 8 Distance between two centers of mass in HSA and cytarabine at 310 K and 313 K

Table 3 Calculation of the binding free energies by the MMPBSA method

Temperature (K)	Vdw. energy (kJ mol^{-1})	Elec. energy (kJ mol^{-1})	Total energy (kJ mol^{-1})
310	-9.24	-26.4	-35.6
313	-7.06×10^{-3}	0.0954	0.0953

indicate the ineffectiveness of cytarabine on the structural change in HSA protein. According to the Fig. 5, it can be seen that the HSA–cytarabine complex at 313 K in 75 ns has a significant increase in the R_g, which indicates the separation of cytarabine from the HSA protein.

Solvent-achievable level specifies the level of a group that is accessible to the solvent. To quantify the effect of cytarabine on HSA protein during the MD simulation process, the available surface solubility (SASA) changes over time. Figure 6 shows the amount of SASA for protein at body temperature and complex at both body temperature and tumor temperature. According to Fig. 6, the amount of SASA in the HSA protein is higher than that of the HSA-cytarabine complex at 310 K, meaning that the HSA protein is gradually exposed to the solvent in the presence of cytarabine, but the access of HSA to the solvent is increased at 313 K, indicating that cytarabine is separated from albumin.

The number of hydrogen bonds and the distance between two centers of mass in protein and drug are shown in Figs. 7 and 8. According to these figures, the number of hydrogen bonds was almost constant during the simulation, but fluctuations were observed in the two regions related to the temperature of 313 K. Figure 7 shows with an increasing simulation time from 45 to 65 ns, the number of hydrogen bonds increased, and between 75 and 80 ns, the number of bonds reached zero, indicating that the protein was moving away from the drug. According to the distance diagram in Fig. 8, a long peak is observed in the time interval of 75 to 80 ns, which indicates that the protein and the drug are separated. But at other times, the distance between the protein and the

Table 4 Occupancy analysis for HSA–cytarabine complex at 310 K

Donor–acceptor	Atom number	Occupancy (%)
LIG-396GLU	18,282–6181	15.2
LIG-400GLU	18,259–6237	22.6
LIG-400GLU	18,259–6236	24.4
LIG-396GLU	18,271–6179	23.6
LIG-396GLU	18,271–6178	29.1
LIG-395PHE	18,271–6166	47.7
LIG-400GLU	6226–18,247	49.2
LIG-400GLU	6226–18,245	29.5

Table 5 Occupancy analysis for HSA–cytarabine complex at 313 K

Donor–acceptor	Atom number	Occupancy (%)
LIG-549ASP	8642–18,271	10.9
LIG-549ASP	8641–18,271	10.8
LIG-540THR	8492 –18,258	12.3
LIG-540THR	8482–18,261	17.7
LIG-413LYS	6474–18,254	12.4
LIG-413LYS	6474–18,247	11.2
LIG-410ARG	6418–18,245	11.0
LIG-410ARG	6412–18,247	15.2
LIG-410ARG	6412–18,245	11.6

drug is a constant value, about 0.2 nm. These results are in good agreement with the results of the number of hydrogen bonds in Fig. 7. According to these two charts, cytarabine as a drug is properly bound to human serum albumin at body temperature, creating a stable complex. However, at 313 K, albumin separates from cytarabine at intervals, which means that the drug is released into the cancer cell at the temperature of the tumor.

The relative binding free energies calculated for the HSA–cytarabine system at temperatures of 310 K and 313 K are estimated by the molecular mechanics Poisson–Boltzmann surface area (MMPBSA)(https://valdes-tresanco-ms.githud.io/gmx_MMPBSA/installation/hth!) method at the final 25 ns of the simulation. This method (MMPBSA) is widely used to calculate the binding free energy between small ligands and biomacromolecules. The various component of this energy is reported in Table 3. Table 3 shows the relative energy conditions for the system. Free energy in general in the connection of the HSA–cytarabine system with a temperature of 310 K,

35.6 kJ mol^{-1} is found to be due to electrostatics and van der Waals. According to the calculated results, the share of van der Waals force in the binding energy is low and electrostatic interactions are the main driving force in the process of binding cytarabine to HSA. The overall change in the energy of the system is negative and indicates the stability of the set. The electrostatic and van der Waals energies are significantly reduced at 313 K compared to 310 K, and the total energy of the HSA–cytarabine system is positive at 313 K, indicating the release of the drug at tumor temperature.

Occupancy analysis was performed for the success of the results of the mentioned graphs and tables. Tables 4 and 5 show the occupancy of amino acids by ligand atoms at 310 K and 313 K, respectively. The first column shows the amino acids of albumin that bonded to the ligand atoms.

The software has a default set number for each of these atoms, shown in the second column. The third column shows the percentage of amino acids occupied by the ligand atoms. Comparing the percentage of occupancy at 313 K and 310 K, it is concluded that amino acids are less occupied by ligand atoms at tumor temperature, indicating that the ligand is separated from the protein at this temperature.

Figure 9 shows the probability of formation of different protein structures in albumin and albumin–cytarabine complexes at temperatures of 310 K and 313 K. The horizontal axis shows the content of various possible protein structures, including Coil, β-sheet, and Bridge-β. As can be seen from Fig. 9, the formation of 5-Helix and Bridge-β is not possible in all three cases, and the structure of α-helix, which is a very important component in the secondary structure of the protein, can be changed in the presence of cytarabine and at different temperatures has no observations.

Fig. 9 Percentage of formation of different protein structures in albumin and albumin–cytarabine complexes at two temperatures of 310 K and 313 K
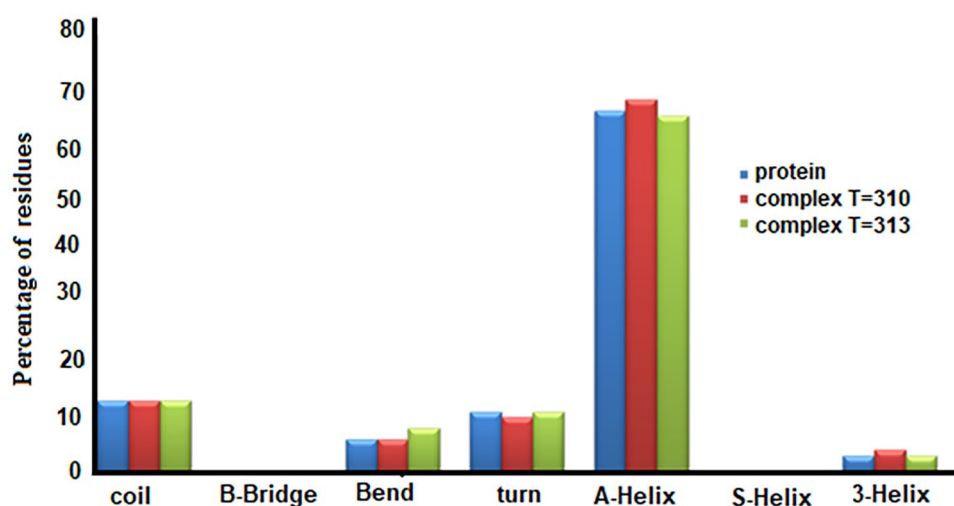
Conclusion

Examination of the simulation results shows that the ligand and protein form a stable and acceptable complex by creating hydrogen bonds and a suitable distance from each other, and the stability of the complex is maintained until the end of the simulation time at body temperature (310 K). In this work, a human serum albumin is a viable option for transporting cytarabine to cancer cells. Because the HSA–cytarabine complex becomes unstable at a temperature of 313 K, the opening of the protein and the reduction of hydrogen bonds occur, resulting in the distance between the drug and the protein. Therefore, it can be concluded that the drug was released at the temperature associated with the cancerous tumor (313 K). Furthermore, we showed human serum albumin is a temperature-sensitive polymer.

Declarations

References

1. Bray F, Ferlay J, Soerjomataram I, Siegel RL, Torre LA, Jemal A (2018) CA Cancer J Clin 68:394–424. https://doi.org/10.3322/caac.21492
2. Nguyen KT (2011) J Nanomed Nanotech 2:103e. https://doi.org/10.4172/2157-7439.1000103e
3. Bharali DJ, Mousa SA (2010) Pharm Ther 128:324–335. https://doi.org/10.1016/j.pharmthera.2010.07.007
4. Senapati S, Mahanta AK, Kumar S, Maiti P (2018) Signal Transduct Target Ther 3:1–19. https://doi.org/10.1038/s41392-017-0004-3
5. Das SK, Menezes ME, Bhatia S, Wang XY, Emdad L, Sarkar D, Fisher PB (2015) J Cell Physiol 230:259–271. https://doi.org/10.1002/jcp.24791
6. Mousa SA, Bharali DJ (2011) Cancers 3:2888–2903. https://doi.org/10.3390/cancers3032888
7. Frangioni JV (2008) J Clin Oncol 26:4012–4021. https://doi.org/10.1200/JCO.2007.14.3065
8. Zaimy MA, Saffarzadeh N, Mohammadi A, Pourghadamyari H, Izadi P, Sarli A, Moghaddam LK, Paschepari SR, Azizi H, Torkamandi S, Tavakkoly-Bazzaz J (2017) Cancer Gene Ther 24:233–243. https://doi.org/10.1038/cgt.2017.16
9. Khan I, Saeed K, Khan I (2019) Arab J Chem 12:908–931. https://doi.org/10.1016/j.arabjc.2017.05.0
10. Rajabi M, Srinivasan M, Mousa SA (2016) Nanobiomaterials in drug delivery, Elsevier Inc, pp. 1–37
11. Peer D, Karp JM, Hong S, Farokhzad OC, Margalit R, Langer R (2007) Nat Nanotech 2:751–760. https://doi.org/10.1038/nnano.2007.387
12. Praetorius NP, Mandal TK (2007) Recent Pat Drug Deliv Formul 1:37–51. https://doi.org/10.2174/187221107779814104
13. Park K (2007) J Control Release 120:1–3. https://doi.org/10.1016/j.jconrel.2007.05.003
14. Yih TC, Al-Fandi M (2006) J Cell Biochem 97:1184–1190. https://doi.org/10.1002/jcb.20796
15. Chatterjee S, Hui PC (2019) Molecules 24:2547–2554. https://doi.org/10.3390/molecules24142547
16. Schattling P, Jochum FD, Theato P (2014) Polym Chem 5:25–36. https://doi.org/10.1039/C3PY00880K
17. Alsuraifi A, Curtis A, Lamprou DA, Hoskins C (2018) Pharmaceutics 10:136–217. https://doi.org/10.3390/pharmaceutics10030136
18. Ding C, Tong L, Feng J, Fu J (2016) Molecules 21:1715. https://doi.org/10.3390/molecules21121715
19. MacEwan SR, Callahan DJ, Chilkoti A (2010) Nanomedicine 5:793–806. https://doi.org/10.2217/nnm.10.50
20. Kost J, Langer R (2001) Adv Drug Deliv Rev 46:125–148. https://doi.org/10.1016/S0169-409X(00)00136-8
21. Torchilin VP (2014) Nat Rev Drug Discov 13:813–827. https://doi.org/10.1038/nrd4333
22. Klouda L, Mikos AG (2008) Eur J Pharm Biopharm 68:34–45. https://doi.org/10.1016/j.ejpb.2007.02.025
23. Langer K, Balthasar S, Vogel V, Dinauer N, von Briesen H, Schubert D (2003) Int J Pharm 257:169–180. https://doi.org/10.1016/s0378-5173(03)00134-0
24. N' soukpoe-Kossi CN (2006) St-Louis C, Beauregard M, Subirade M, Carpentier R, Hotchandani S, Tajmir-Riahi HA. J Biomol Struct Dyn 24:277–283. https://doi.org/10.1080/07391102.2006.10507120
25. Jahanban-Esfahlan A, Dastmalchi S, Davaran S (2016) Int J Biol Macromol 91:703–709. https://doi.org/10.1016/j.ijbiomac.2016.05.032
26. Roy A, Seal P, Sikdar J, Banerjee S, Haldar R (2018) J Biomol Struct Dyn 36:387–397. https://doi.org/10.1080/07391102.2017.1278721
27. Salci A, Toprak M (2017) J Biomol Struct Dyn 35:8–16. https://doi.org/10.1080/07391102.2015.1128357
28. Silva D, Cortez CM, Cunha-Bastos J, Louro SRW (2004) Toxicol Lett 147:53–61. https://doi.org/10.1016/j.toxlet.2003.10.014
29. Kratz F (2008) J Control Release 132:171–183. https://doi.org/10.1016/j.jconrel.2008.05.010
30. Xu L, Hu YX, Li J, Liu YF, Zhang L, Ai HX, Liu HS (2017) J Photochem Photobiol B 173:187–195. https://doi.org/10.1016/j.jphotobiol.2017.05.039
31. Rahnama E, Mahmoodian-Moghaddam M, Khorsand-Ahmadi S, Saberi MR, Chamani J (2015) J Biomole Struct Dyn 33:513–533. https://doi.org/10.1080/07391102.2014.893540
32. Sleep D (2015) Expert Opin Drug Deliv 12:793–812. https://doi.org/10.1517/17425247.2015.993313
33. Peters JrT (1995) All about albumin: biochemistry, genetics, and medical applications, 1st edition, Academic Press; 1st edition
34. Neumann E, Frei E, Funk D, Becker MD, Schrenk H-H, Muller-Ladner U, Fiehn C (2010) Expert Opin Drug Deliv 7:915–925. https://doi.org/10.1517/17425247.2010.498474
35. Hoogenboezem EN, Duvall CL (2018) Adv Drug Deliv Rev 130:73–89. https://doi.org/10.1016/j.addr.2018.07.011
36. Charbon V, Latour I, Lambert DM, Buc-Calderon P, Neuvens L, De Keyser JL (1996) Pharm Res 13:27–31. https://doi.org/10.1023/a:1016012913664
37. Wolfrum C, Shi S, Jayaprakash KN, Jayaraman M, Wang G, Pandey RK, Rajeev KG, Nakayama T, Charrise K, Ndungo EM, Zimmermann T, Koteliansky V, Manoharan M, Stoffel M (2007) Nat Biotechnol 25:1149–1157. https://doi.org/10.1038/nbt1339
38. Karimi M, Bahrami S, Baghaee Ravari S, Sahandi Zangabad P, Mirshekari H, Bozorgomid M, Shahreza S, Sori M, Hamblin MR (2016) Expert Opin Drug Deliv 13:1609–1623

39. Peters T Jr (1985) Adv Protein Chem 37:161–245. https://doi.org/10.1016/S0065-3233(08)60065-0
40. Yokoyama M, Okano T (1996) Adv Drug Deliv Rev 21:77–80. https://doi.org/10.1016/S0169-409X(96)00439-5
41. Walwick ER, Dekker CA, Roberts WK (1959) Proc Chem Soc Lond 3:84. https://doi.org/10.1039/PS9590000073
42. Adamson PC (2015) CA Cancer J Clin 65:212–220. https://doi.org/10.3322/caac.21273
43. Malani D, Murumägi A, Yadav B, Kontro M, Eldfors S, Kumar A, Karjalainen R, Majumder MM, Ojamies P, Pemovska T (2017) Leukemia 31:1187–1195. https://doi.org/10.1038/leu.2016.314
44. Purich DL (2018) The inhibitor index: a desk reference on enzyme inhibitors, receptor antagonists, drugs, toxins, poisons, biologics, and therapeutic leads. Taylor & Francis, CRC Press
45. Kojima H, Iida M, Miyazaki H, Koga T, Moriyama H, Manome Y (2002) Arch. Otolaryngol Head Neck Surg 128:708–713. https://doi.org/10.1001/archotol.128.6.708
46. Zaboli M, Raissi H, Rahmani Moghaddam N, Farzad F (2020) J Mol Liq 301:112458. https://doi.org/10.1016/j.molliq.2020.112458
47. Deepa G, Sivakumar KC, Sajeevan TP (2018) 3 Biotech. 8:493. https://doi.org/10.1007/s13205-018-1510-x
48. Baker WJ, Royer GL Jr, Weiss RB (1991) J Clin Oncol 9:679–693. https://doi.org/10.1200/JCO.1991.9.4.679
49. Ho DHW, Frei E (1971) Clin Pharmacol Ther 12:944–954. https://doi.org/10.1002/cpt1971126944
50. Yadav MK, Ahmad S, Raza K, Kumar S, Eswaran M, KM MP(2023) J Biomol Struct Dyn 41: 1527–1539. https://doi.org/10.1080/07391102.2021.2021993
51. Karwasra R, Ahmad S, Bano N, Qazi S, Raza K, Singh S, Varma S (2022) Molecules 27:6034. https://doi.org/10.3390/molecules27186034
52. Ahmad S (2022) KM MP, Raza K, Rafeeq MM, Habib AH, Eswaran M, Yadav MK. J Biomol Struct Dyn 22:1–11. https://doi.org/10.1080/07391102.2022.2060308
53. Alturki NA, Mashraqi M, Alzamami A, Alghamdi YS, Alharthi AA, Asiri S, Ahmad S, Alshamrani S (2022) Molecules 27:6034. https://doi.org/10.3390/molecules27144391
54. Ahmad S, Bano N, Qazi S, Yadav MK, Ahmad N, Raza K, (2022) Nat Prod Commun, 1934578X221115499 https://doi.org/10.1177/1934578X221115499
55. Pires DEV, Blundell TL, Ascher DB (2015) J Med Chem, 2015; 58(9):4066–72. https://doi.org/10.1021/acs. Jmedchem.5b00104
56. Jafari F, Samadi S, Nowroozi A, Sadrjavadi K, Moradi S, Ashrafi-Kooshk MR, Shahlaei M (2018) J Biomol Struct Dyn 36:1490–1510. https://doi.org/10.1080/07391102.2017.1329096
57. Doss CGP, Chakraborty C, Chen L, Zhu H (2014) BioMed Res Int 895831–14. https://doi.org/10.1155/2014/895831